Experiments on the Dynamic Behavior of the Chemical Looping Combustion Process

Lennard Lindmüller[1,*], Johannes Haus[2], and Stefan Heinrich[1]

DOI: 10.1002/cite.202200155

Dedicated to Prof. Dr.-Ing. Joachim Werther on the occasion of his 80th birthday

The dynamic operation of thermal power plants becomes more and more important due to more diverse and volatile power sources. Load changes of biomass, bituminous coal and methane were conducted during six experimental runs in a chemical looping combustion pilot plant which combines power generation and CO_2 capture. The resulting step responses of the hydrodynamics and gas concentrations were compared to each other to understand the transient behavior of the interconnected fluidized bed system. The influence of the fuel rate and solid circulation on the response time and intensity was assessed.

Keywords: Chemical looping combustion, Circulating fluidized bed, Process dynamics

Received: July 31, 2022; *revised:* November 09, 2022; *accepted:* November 29, 2022

1 Introduction

The introduction of renewable energy towards the electric power system is a challenge due to the volatility of the power output of solar and wind power. This led to considerable price differences of electricity on the European energy market in the last decade. To help stabilize the power grid and be able to monetarize on the price fluctuations, a dynamic analysis of conventional power plants fired with coal, waste or biomass is indicated. Even the transmission system operators demand that conventional power plants have the capability to release reserve power on different time scales into the grid on request [1]. Therefore, several industrial stakeholders and researchers in academia investigated the flexibilization of coal fired power plants and the involved upstream and downstream equipment. For novel power generation technologies with carbon capture this system demands will still be valid. From our point of view, it will also be from utmost importance how such systems behave with regards on CO_2 quality for sequestration, like concentration of CO_2 and other gases in the exhaust, during load changes as well as shutdown and start-up. Wellner et al. [2] found out with a combined simulation of a coal fired plant and a subsequent post combustion capture that the capture unit reaches peak capacity after more than 30 min and that results from dynamic simulations can lower the steam demand of the capture technology. Hentschel et al. [3] conducted a dynamic simulation of a 550 MW_{el} coal fired power plant and validated it against plant data at part load and full load. Additionally, load changes were investigated which showed that the model can capture several operation parameters accurately. With the help of the model, the system control should be improved to allow for higher load changes. This is not solely a European problem, what can be seen by the work in the U.S., for example by Sarda et al. [4], who developed a dynamic model of a supercritical pulverized coal power plant in Aspen Plus Dynamics and Aspen Custom Modeler. This was again done to improve the plants control system towards load-changes. Looking into the Asian energy market, one can also find plenty of research going into the flexibilization of coal fired power plants. Wang et al. [5] for example, conducted a thermodynamic study of a 660 MW unit to improve the coal feed rate during the start-up and shutdown.

At Hamburg University of Technology (TUHH), the chemical looping combustion (CLC) process is investigated both with modeling work and also with the help of a 25 kW_{th} pilot plant for solid and gaseous fuels. The process consists of at least two reactors, an air reactor, where the oxidizing air is introduced and a fuel reactor, where the fuel is inserted. Between both reactors, a solid oxygen carrier (OC) is circulated, which is oxidized in the air reactor by the oxygen and reduced in fuel reactor by the gaseous or gasified fuel [6]. This can lead to a highly efficient CO_2 sequestration process, as the energy intensive pre- or post-combustion gas treatment

[1]Lennard Lindmüller https://orcid.org/0000-0001-7278-8392, Prof. Dr.-Ing. habil. Dr. h.c. Stefan Heinrich (lennard.lindmueller@tuhh.de)
Hamburg University of Technology, Institute of Solids Process Engineering and Particle Technology, Denickestraße 15, 21073 Hamburg, Germany.

[2]Dr. Johannes Haus
BASF SE, Carl-Bosch-Straße 38, 67056 Ludwigshafen, Germany.

is avoided. A CLC system usually is made up from a circulating fluidized bed (CFB) riser as air reactor and a bubbling or circulating fluidized bed as fuel reactor. Dynamic investigations on the process are rare. One can find Bayham et al. [7], which looked at the gas concentration development during the start-up and shutdown of a CLC plant.

The dynamic behavior of circulating fluidized beds itself was investigated by Hartge et al. [8], who developed a dynamic population balance-based model of the hold-up bed mass in a system and they were able to describe long-term effects of attrition in such systems seen in a pilot scale combustor. Peters et al. [9] looked experimentally into the coal combustion inside a 1 MW_{th} large pilot scale unit during load changes. Their 1.5-dimensional model of the circulating fluidized bed was able to capture the hydrodynamics and temperature distribution and, with it, give insight into the systems behavior during the load changes.

What is still missing is an experimental validation scenario for the dynamic simulations taking into consideration the hydrodynamic effects in the fluidized bed system and the influence of solid circulation on the gas conversion of the involved reactive solids. In this work, we present an experimental analysis of a CLC system based on measurements of the hydrodynamics and gas concentration measurements with a special focus on the dynamics and the timescales of the respective phenomena investigated. In this work six experimental runs are compared to their response behavior of fuel load changes. Three runs with biomass, two with bituminous coal and one with methane. The experiments were conducted on the 25 kW_{th} pilot plant at TUHH. The progressions of the gas concentrations in the air reactor are presented as a step response of a first order system. This way the systems' responses are made comparable and differences of the conversion behavior of the different fuels can be derived.

2 Materials and Methods

2.1 Experimental Facility

A 25 kW_{th} CLC pilot plant is operated at TUHH. Fig. 1 shows the schematics of the pilot plant with a two-stage bubbling bed FR system. The facility consists of an air reactor (AR), fuel reactor (FR), the upper loop seal (S1), the lower loop seal (S2), standpipes (SP1–SP3) and a cyclone. As a special design, the TUHH CLC plant was designed with a two-stage FR system, the lower FR stage 1 and the upper FR stage 2. The two stages are connected via the standpipe SP2. For process control, online measurements of pressure drop, temperature are conducted all over the system.

Gas measurements ports are at the exit of the AR separation cyclone and the FR2 exit. The FR2 outlet measurement can be temporarily switched to take gas out of the first stage FR1. The plants dimensions are shown in Tab. 1. The entire CLC reactor is jacketed and fitted with electric heating, which can heat the system up to 1000 °C. The lower loop

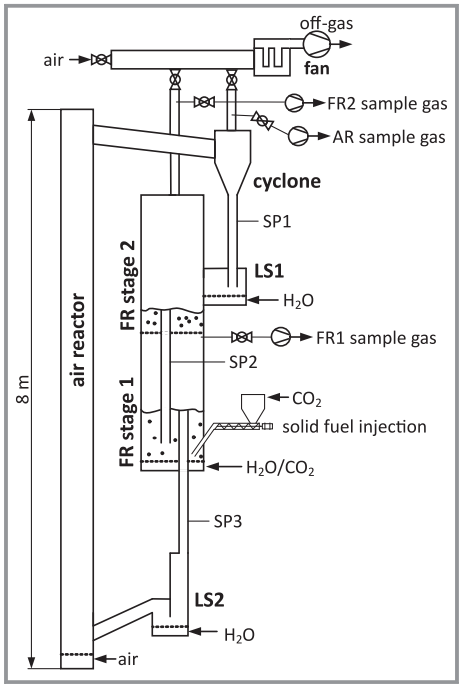

Figure 1. Schematics of the 25 kW_{th} CLC pilot-plant at Hamburg University of Technology (AR: air reactor, FR: fuel reactor, LS1 and LS2: loop seals, SP1-3: standpipes).

seal LS2 is connected to the lower FR stage via the lower standpipe SP3 preventing the back flow of gases from AR to FR. At the lower loop seal LS2 there is the possibility to extract solid samples, which can be used to determine the oxidation state of the circulated oxygen carrier. The upper loop seal LS1 is connected to the cyclone via the upper standpipe SP1. It prevents the back flow of gases from FR upper stage to the cyclone exit.

Table 1. Inner dimensions of the CLC facility.

	height [m]	diameter [m]
riser air reactor	8	0.1
fuel reactor height per stage	2	0.25
bed height stage 1	0.6	–
bed height stage 2	0.3	–
standpipe SP1	1	0.07
standpipe SP2	2.5	0.07
standpipe SP3a	1.5	0.07
standpipe SP3b	1	0.11
loop seal 1	width 0.16	length 0.13
loop seal 2	width 0.2	length 0.25
cyclone	0.34	0.21 (barrel); 0.067 (cone tip)

2.1.1 Online Measurement Systems

With an online gas measurement system, gas concentrations are measured in fuel reactor stage 1 or stage 2 and in the air reactor. A description of the whole gas measurement system can be found in a previous publication [10]. The focus in this work are the gas concentrations at the air reactor exit. The sampling port is at the exit of the cyclone. Oxygen concentrations are measured with an electrochemical analyzer (Oxynos 100, Leybol-Heraeus) between 0–25 vol %. Carbon dioxide is measured via non-dispersive infrared diffraction (NDIR) (Gas Card, Edinburgh Instruments, Ltd.) between 0–30 vol %.

2.2 Material

The CLC facility is operated with CuO/Al_2O_3 oxygen carrier with 9 wt % CuO, which was fabricated by impregnating γ-alumina (Puralox® NWa-155 by Sasol) with a solution of copper nitrate. A method introduced by de Diego et al. [11] was used. Tab. 2 summarizes the main properties of the oxygen carrier. The properties of the solid fuels are summarized in Tab. 3. Detailed descriptions of the used fuels are found in the previous works for softwood [12], hardwood [13], methane [14], bituminous coal [10].

Table 2. Characterization of the oxygen carrier CuO/Al_2O_3 in the CLC facility.

Parameter	Value
ρ_s [kg m^{-3}]	4094
ρ_{bulk} [kg m^{-3}]	1027
d_{sauter} [µm]	286
u_{mf} [m s^{-1}]	0.042

Table 3. Solid fuel properties.

	softwood	hardwood	bituminous coal
d_{sauter} [mm]	0.73	1.082	0.233
bulk density [kg m^{-3}]	245	354	1400
lower heating value [MJ kg^{-1}]	18.53	18.7	26.7

2.3 Experimental Procedure

The CLC system was operated with the following fuel types on six measurement days: Two with identical softwood, one with hardwood, two with identical bituminous coal and one with methane. At a temperature of 850 °C fuel load changes were applied during those runs. The second run with bituminous coal was conducted at 900 °C. The fuel loads were changed between 0 kg h^{-1} up to 5.5 kg h^{-1} ramping up the system's thermal input from 0 kW_{th} up to 28 kW_{th} depending on the used fuel. The applied load changes are shown in Tab. 3. It is assumed that the fuel load change happens instantaneously as the used system of screw conveyor is filled with fuel during start of the load change. During the operation, online gas measurements were conducted as well as pressure measurements.

Additionally, after one load change with methane and one with lignite as fuel, solid samples were taken before the fuel load change and then after 2, 4, 6, 8, 10 and 12 min of operation to see a change of the oxygen carrier conversion. The results with lignite as fuel could not be evaluated for this work due to issues with the gas measurement system during this experimental run.

The solid oxygen carrier has a certain ability to carry oxygen, called oxygen carrying capacity or R_0. Based on the principle of the R_0 determination of the oxygen carrier, the samples from the dynamic operation are analyzed similarly to Thon [15]. The various material samples are weighed and selectively reduced or oxidized using a thermogravimetric analysis (TGA) at a target temperature of 850 °C. First a separate solid sample is completely oxidized by oxygen and completely reduced by hydrogen in the TGA to create a reference, which gives also the oxygen carrying capacity R_0. Later, the samples from the dynamic pilot operation can be compared to the reference data of the same used carrier. This way also the oxygen carrier conversion is determined.

3 Data Evaluation

3.1 Control Theory

To better describe the dynamic behavior of the combustion system and to compare different experimental runs, it was decided to use ideas from control theory. For that, the signal theory from system control textbooks by Döring [16] and Unbehauen [17] is used and applied to the combustion system. The response to a step function is well suited to determine the time response of the pressure drops and gas concentrations since both signals reach a new steady state without any significant overshoot. A PT1 system is characterized by a proportional time delayed response, where the delay is of first order. The response signal $v(t)$ can be described by the following:

$$v(t) = K\left(1 - e^{-\frac{t}{\tau_{63}}}\right)\Delta u \tag{1}$$

In the function τ_{63} is the time at which the response function reaches 63 % of its final value and t is the actual time. The gain factor K is defined as the ratio of the change of the output function Δy to the input function Δu as shown in Eq. (2):

$$K = \frac{\Delta y}{\Delta u} \quad (2)$$

This model is a simplification since no overshoot height of the response signal are described. In this work, Eq. (1) describes the course of the gas concentrations in the air reactor as a PT1 system with the fuel inlet rate as the input function. The first order response was fitted as close as possible to the experimental data by adjusting the gain factor K and process time constant τ_{63}. By determining K and τ_{63} for all experimental data an effective comparison of the step responses could be conducted. For a better understanding of the transient response behavior from a process engineering perspective, the transition times from one steady state to another $t_{\text{steady state}}$ were also determined for all process changes.

4 Results and Discussion

4.1 Response Time of the Systems Hydrodynamics

Exemplarily, Fig. 2 shows the outlet gas concentrations of CO_2 and O_2 in the air reactor as well as the pressure drop of the whole riser air reactor after starting a fuel injection into the system during the combustion of softwood. Increasing the fuel rate leads to a lower oxygen concentration in the air reactor since more oxygen carrier needs to be reoxidized. Higher carbon dioxide concentrations are measured due to a carbon slip from fuel reactor to air reactor. The higher the fuel rate, the more char is transported into the air reactor with oxygen carrier particles. The dotted lines show the courses of measured data, represented as first order step responses.

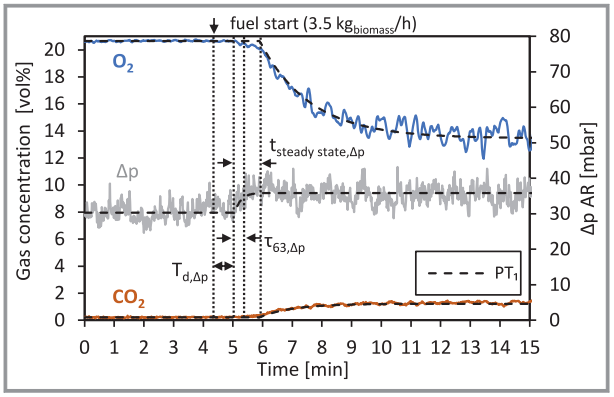

Figure 2. Experimental values and representation of step response as first order system (PT1) of the pressure drop and gas concentrations in the air reactor before and after adding 3.5 $kg_{biomass}h^{-1}$ fuel to the system ($T_{d,\Delta p}$ = dead time, $\tau_{63\Delta p}$ = process time constant of the pressure drop).

Adding fuel to the system leads to an increase of gas velocities in the fuel reactor due to the generation of gases. In the air reactor, the gas velocity decreases due to the conversion of oxygen. This leads to a balancing of the pressures in the entire system, which explains the shorter dead time of the pressure drop compared to the gas concentrations. The pressure drops of the first and second fuel reactor adapt even faster since the fuel is directly fed into the bed of the first fuel reactor stage. The dead time, gain factor K, process time constant τ_{63} and $t_{\text{steady state}}$ for this set of data are shown in Tab. 4. The dead times of the gas concentrations were the same, while the process time constant and the time to reach a new steady state time were longer for oxygen. The latter effect is explained in more detail in the next section.

Table 4. Dead times T_d, process time constants τ_{63}, $t_{\text{steady state}}$ and gain factors K for the pressure drop and gas concentrations in the air reactor for a fuel load change of softwood of 0 → 3.5 $kg\,h^{-1}$.

	T_d [min]	τ_{63} [min]	$t_{\text{steady state}}$ [min]	K [vol % (kg/h)$^{-1}$]
O_2	1.6	1.7	7.83	−2.06
CO_2	1.6	1.1	4.52	0.28
Δp AR	0.7	0.3	0.6	1.77

4.2 Step Responses

Tab. 5 shows the transition times from one steady state to another $t_{\text{steady state}}$, the process time constants τ_{63} and gain factors K for O_2 and CO_2 concentrations in the air reactor for different fuel load changes. The experimental data was obtained on six measurement days: Two with identical softwood, one with hardwood, two with identical bituminous coal and one with methane.

Exemplarily, data sets of the step responses of the gas concentrations in the air reactor for softwood 1, bituminous coal 1 and methane are presented in Fig. 3. For the methane conversion, no CO_2 is detected in the air reactor because the carbon slip only occurs for solid fuels with a significant amount of fixed carbon.

4.3 Step Response Interpretation

For all used solid fuels, the gain factor K increases for higher fuel rates, which means that, e.g., by equally increasing the fuel rate two times, the second increase would lead to a higher relative conversion of O_2 or generation of CO_2 in the air reactor. Exemplary increases of the fuel rate of softwood 2 from 0 to 0.9 $kg\,h^{-1}$ and 0.9 to 1.8 $kg\,h^{-1}$ lead to a K_{O2} of 1.56 and 2.4. This effect occurs because for higher fuel rates unconverted char is transported into the air reactor with the oxygen carrier. There it is converted by oxygen, which further decreases the oxygen concentration in the air reactor. Generally, this effect is much smaller for lower fuel inlet rates [10], for smaller fuel sizes and for fuels with lower amounts of fixed carbon (e.g., biomass) [12].

Table 5. Transition times from one steady state to another $t_{steady\,state}$, process time constants τ_{63}, and gain factors K for O_2 and CO_2 in the air reactor of different fuel types for different fuel load changes (n.a. = not available due to temporal issues in gas measurement system, e.g., purging and removal of condensate water).

Fuel	fuel load change		$t_{steady\ state}$ [min]	$\tau_{63,O2}$ [min]	K_{O2} [vol % (kg/h)$^{-1}$]	$t_{steady\ state}$ [min]	$\tau_{63,CO2}$ [min]	K_{CO2} [vol % (kg/h)$^{-1}$]
	[kg h^{-1}]	[kW$_{th}$]						
Softwood 1	0 → 3.5	17.8	7.83	1.7	–2.1	4.52	1.1	0.28
	3.5 → 5.5	28	7.8	2	–3.7	2.9	0.45	0.81
	5.5 → 0	0	6.2	1.3	–2,5	4.9	1	1.0
	0 → 3.5	17.8	7.3	1.5	–1.7	3.92	1.1	0.26
	3.5 → 5.5	28	7.4	1.5	–3.4	3.12	0.8	0.57
Softwood 2	0 → 0.9	4.6	13.1	4	–1.6	5.1	1.5	0.13
	0.9 → 1.8	9.3	11.7	4.5	–2.4	3.6	2.5	0.22
	1.8 → 3	15.4	9.59	2	–3.7	5.5	1	0.56
	3 → 0	0	8.05	1.5	–2.5	3.75	0.5	0.33
	0 → 1	5.1	11.9	2	–1.9	2.32	0.6	0.15
	1 → 1.5	7.7	6.3	1	–2.2	2.834	0.5	0.20
	1.5 → 3	15.4	12.6	2.5	–2.5	4.067	0.8	0.33
	3 → 3.8	19.6	7.6	1	–3.5	1.15	0.1	1.18
Hardwood	0 → 2.4	15.3	n.a.	n.a.	–1.9	n.a.	n.a.	0.20
	2.4 → 3.1	19.1	8.6	3.5	–3.9	n.a.	n.a.	0.11
	3.1 → 0	0	13.2	2.4	–2.3	4.71	0.75	0.1
	0 → 3.1	15.3	19.2	4.1	–2.3	4.51	1	0.09
	3.1 → 0	19.1	8.68	2.4	–2.3	2.85	0.75	0.1
Bituminous coal 1	1.4 → 0	0	14.8	3.2	–3.7	10.6	3	1.47
	0 → 1.4	10.2	19.6	3.9	–3.7	15.21	3	1.43
	1.4 → 2.5	17.8	21.4	6.0	–4.5	15.46	5	1.5
	2.5 → 3.7	26.7	22.9	6.5	–4.4	16.8	6	1.38
	3.7 → 0	0	11.6	3.3	–4.3	9	3.3	1.43
Bituminous coal 2	2.2 → 3	22.25	8.25	2.4	–2.2	n.a.	n.a.	n.a
	3 → 3.8	28.2	9.1	4	–4.2	4.47	2.8	0.71
	3.8 → 0	0	7.3	2	–3.9	5.54	1.5	0.95
Methane	0 → 1.1	15.3	14.3	4.5	–6.1	–	–	–
	1.1 → 0	0	12.7	4	–5.9	–	–	–

By comparing all measurements, it can be concluded, that the fuel input rate does not have a clear effect on the process time constant τ_{63} as no obvious trend between those two can be observed. The same goes for the time to reach a new steady state $t_{steady\,state}$. This is on the first look counter intuitive since one can assume that a higher fuel inlet rate would lead to a longer response time of the system, due to slower solid fuel reaction rates and more unfavorable gas compositions in the system. An explanation is that a higher fuel input leads to higher gas flows and with it, a higher expansion of the fluidized beds, which leads to an increased solid circulation, as shown in a previous work [18]. A higher circulation rate transports the particles faster from fuel to air reactor. Therefore, a higher solid circulation rate could further decrease the transition times.

In average, the process time constant τ_{63} is reached 2.15 times faster and $t_{steady\,state}$ is reached 2.26 times faster for CO_2 compared to O_2. This can be explained with the fact

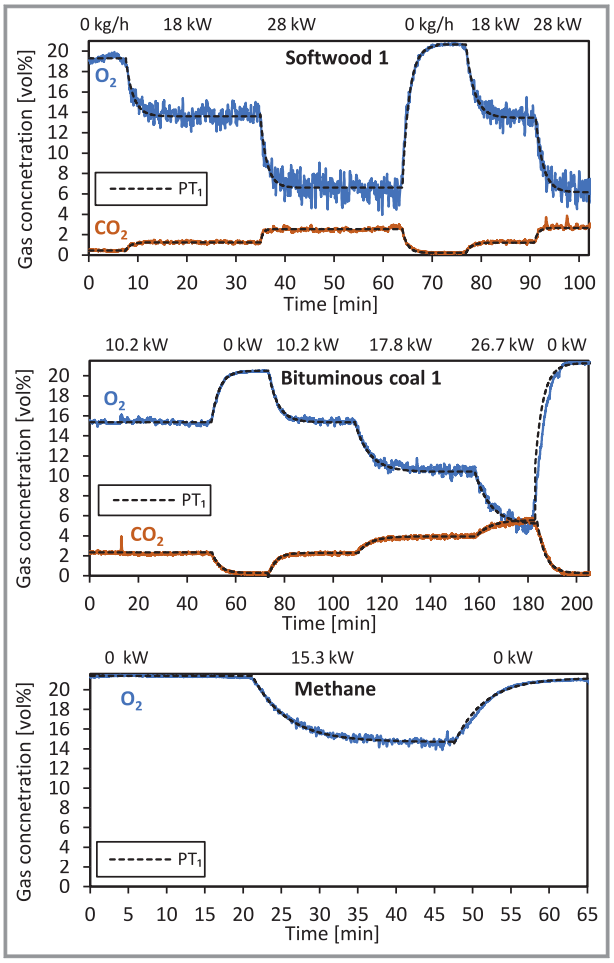

Figure 3. Measured course and first order step responses of the O_2 and CO_2 concentrations in the air reactor after changing the fuel load (PT1: representation of step response in first order system).

that the CO_2 concentration in the air reactor only depends on the char conversion in the fuel reactor and subsequently on the carbon slip. The O_2 concentration on the other side depends additionally on the conversion state of the oxygen carrier coming from the fuel reactor. The oxygen carrier reacts with the fuel gas by entering the second stage. The material then needs to pass the first stage and then a loop seal to enter the air reactor. Solid fuels on the other side are fed into the bed of the first fuel reactor stage, which means that they leave the fuel reactor earlier than oxygen carrier particles which are affected by the conversion. In most experimental runs, decreasing the fuel rate led to shorter transition times to a new steady state than increasing the fuel rate. This was expected since the reoxidation of the oxygen carrier particles in the air reactor is considerably faster than the reactions in the fuel reactor [19].

4.4 Oxygen Carrier Conversion

Oxygen carrier samples were collected from the lower loop seals during load changes of two experimental runs, using lignite and methane. Those samples were extracted from the lower loop seal in hot conditions with a cooled, nitrogen purged container. By taking a sample every two minutes, the conversion of the oxygen carrier X_s after leaving the fuel reactor could be assessed over time during the load changes. Fig. 4 shows the oxygen carrier conversion X_s after starting and stopping the injection of methane (15.3 kW_{th}) and lignite (18.2 kW_{th}). Above the graph, pictures of the oxygen carrier samples at each conversion state during the lignite combustion are seen. Different oxidation states are clearly observable by the color change from khaki to a dark grey and back. The oxygen carrier reaches a conversion of 0.27 with methane and 0.32 with lignite. For both fuels a new

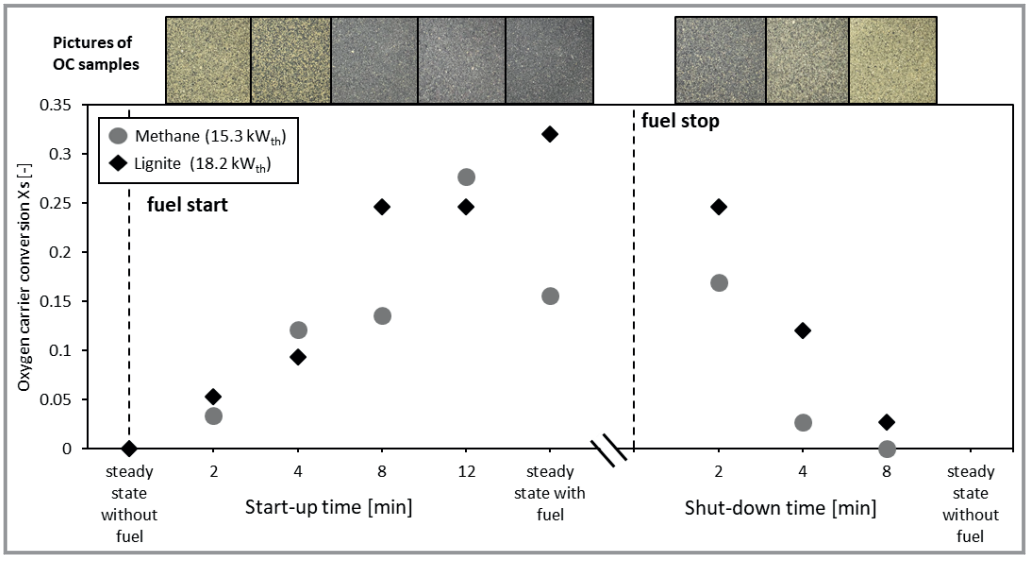

Figure 4. Oxygen carrier conversion X_s after starting and stopping a fuel injection of methane and lignite coal. Top: Pictures of the oxygen carrier at specific conversion state with lignite.

steady state is achieved within 12–14 min after adding fuel and 10 min after stopping the fuel rate. This corresponds to the findings presented in the previous section.

5 Conclusion

In this work, an assessment of response time after applying fuel load changes in a 25 kW_{th} chemical looping combustion system for biomass, bituminous coal and methane was conducted. All courses of the gas concentrations in the air reactor were presented as step responses of a first order system to make an effective comparison between the different experiments. The systems hydrodynamics adapted within one minute in both fuel reactor and air reactor after a load change. The response in the fuel reactor was even shorter. There was no time dependency of the load change intensity on the transition time to another steady state in the used CLC system at given rates. This means that a change from 2 to 3.6 $kg\,h^{-1}$ had a similar transition time as a load change from 0 to 3.6 $kg\,h^{-1}$. The system dynamics are mostly dependent on fluid mechanics, which influence the solid circulation. The solid circulation is the key driver for transferring the oxygen carrier in the system and reaching a new steady state. The CLC system response of the gas concentrations after fuel load decreases were always shorter than for fuel load increases. In the used CLC facility, the transition time of the CO_2 concentration in the air reactor after a solid fuel load change is average 2.2 times faster than for the oxygen concentration.

Open access funding enabled and organized by Projekt DEAL.

Symbols used

d_{sauter}	[mm]	Sauter mean diameter
K	[vol % $(kg/h)^{-1}$]	gain factor
R_0	[%]	oxygen carrying capacity
T_d	[min]	dead time
$t_{steady\ state}$		[min] transition times from one steady state to another
X_s	[–]	oxygen carrier conversion

Greek letters

τ_{63}	[min]	process time constant
ρ_{bulk}	[$kg\,m^{-3}$]	bulk density
ρ_s	[$kg\,m^{-3}$]	solid density

Abbreviations

CFB Circulating Fluidized Bed
CLC Chemical Looping Combustion
TGA Thermogravimetric Analysis

References

[1] H. Khajeh, H. Laaksonen, A. S. Gazafroudi, M. Shafie-khah, *Energies* **2020**, *13 (1)*, 165. DOI: https://doi.org/10.3390/en13010165
[2] K. Wellner, T. Marx-Schubach, G. Schmitz, *Ind. Eng. Chem. Res.* **2016**, *55 (46)*, 12038–12045. DOI: https://doi.org/10.1021/acs.iecr.6b02752
[3] J. Hentschel, H. Zindler, H. Spliethoff, *Energy* **2017**, *137*, 927–940. DOI: https://doi.org/10.1016/j.energy.2017.02.165
[4] P. Sarda, E. Hedrick, K. Reynolds, D. Bhattacharyya, S. E. Zitney, B. Omell, *Processes* **2018**, *6 (11)*, 226. DOI: https://doi.org/10.3390/pr6110226
[5] C. Wang, M. Liu, B. Li, Y. Liu, J. Yan, *Energy* **2017**, *122*, 505–527. DOI: https://doi.org/10.1016/j.energy.2017.01.123
[6] A. Lyngfelt, B. Leckner, T. Mattisson, *Chem. Eng. Sci.* **2001**, *56 (10)*, 3101–3113. DOI: https://doi.org/10.1016/S0009-2509(01)00007-0
[7] S. Bayham, O. McGiveron, A. Tong, E. Chung, M. Kathe, D. Wang, L. Zeng, L.-S. Fan, *Appl. Energy* **2015**, *145*, 354–363. DOI: https://doi.org/10.1016/j.apenergy.2015.02.026
[8] E.-U. Hartge, C. Klett, J. Werther, *Chem. Eng. Sci.* **2007**, *62 (1–2)*, 281–293. DOI: https://doi.org/10.1016/j.ces.2006.08.067
[9] J. Peters, F. Alobaid, B. Epple, *Appl. Sci.* **2020**, *10 (17)*, 5972. DOI: https://doi.org/10.3390/app10175972
[10] J. Haus, K. Lyu, E.-U. Hartge, S. Heinrich, J. Werther, *Energy Technol.* **2016**, *4 (10)*, 1263–1273. DOI: https://doi.org/10.1002/ente.201600102
[11] L. F. de Diego, P. Gayán, F. García-Labiano, J. Celaya, A. Abad, J. Adánez, *Energy Fuels* **2005**, *19 (5)*, 1850–1856. DOI: https://doi.org/10.1021/ef050052f
[12] L. Lindmüller, J. Haus, S. Heinrich, *Energy Fuels* **2022**, *36*, 9529–9537. DOI: https://doi.org/10.1021/acs.energyfuels.2c00901
[13] J. Haus, L. Lindmüller, T. Dymala, K. Jarolin, Y. Feng, E.-U. Hartge, S. Heinrich, J. Werther, *Mitigation Adapt. Strategies Global Change* **2020**, *25 (6)*, 969–986. DOI: https://doi.org/10.1007/s11027-020-09917-2
[14] J. Haus, E.-U. Hartge, S. Heinrich, J. Werther, *Int. J. Greenhouse Gas Control* **2018**, *72*, 26–37. DOI: https://doi.org/10.1016/j.ijggc.2018.03.004
[15] A. Thon, *Operation of a system of interconnected fluidized bed reactors in the chemical looping combustion process*, 1st ed., SPE-Schriftenreihe, Vol. 1, Cuvillier, Göttingen **2014**.
[16] D. Döring, *Eine kurze Einführung in die Systemtheorie: Lehr- und Übungsbuch*, Springer eBook Collection, Vieweg+Teubner Verlag, Wiesbaden **2011**.
[17] R. Unbehauen, *Systemtheorie 1: Allgemeine Grundlagen, Signale und lineare Systeme im Zeit- und Frequenzbereich*, 8th ed., De Gruyter, München **2002**.
[18] L. Lindmüller, J. Haus, A. Ramesh Kumar Nair, S. Heinrich, *Chem. Eng. Sci.* **2022**, *250*, 117366. DOI: https://doi.org/10.1016/j.ces.2021.117366
[19] T. Mattisson, M. Johansson, A. Lyngfelt, *Energy Fuels* **2004**, *18 (3)*, 628–637. DOI: https://doi.org/10.1021/ef0301405

DOI: 10.1002/cite.202200155

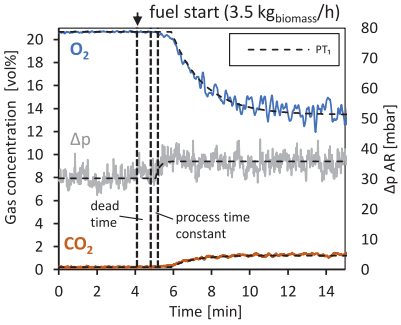

Experiments on the Dynamic Behavior of the Chemical Looping Combustion Process

Lennard Lindmüller, Johannes Haus, Stefan Heinrich*

Research Article: Chemical looping combustion combines power generation and CO_2 capture. In a pilot plant, load changes with biomass, coal and methane were conducted to understand the transient behavior of the interconnected fluidized bed system. An evaluation of the fuel load and circulation rate on the response time response time and intensity was performed.

